Conformational Dynamics of the Partially Disordered Yeast Transcription Factor GCN4

Paul Robustelli†, Nikola Trbovic†, Richard A. Friesner§, and Arthur G. Palmer III†

†Department of Biochemistry and Molecular Biophysics, Columbia University, New York NY 10032, USA

§Department of Chemistry, Columbia University, New York NY 10027, USA

Supporting Information

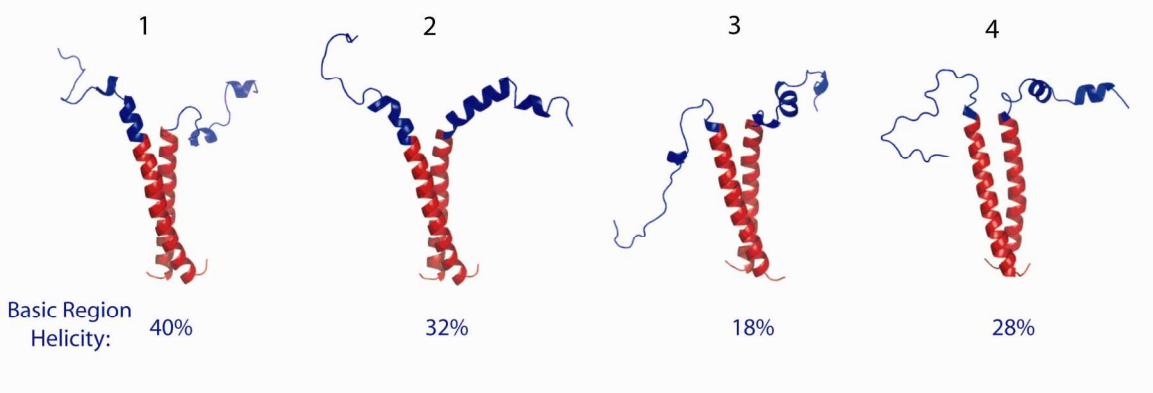

SI Figure 1. GCN4 bZip domain starting structures used for 100 ns NVT production MD trajectories. Residues in the basic region (1-25) are colored blue and residues in the leucine zipper (26-56) are colored red. The percent helicity of the basic region is noted beneath each structure.

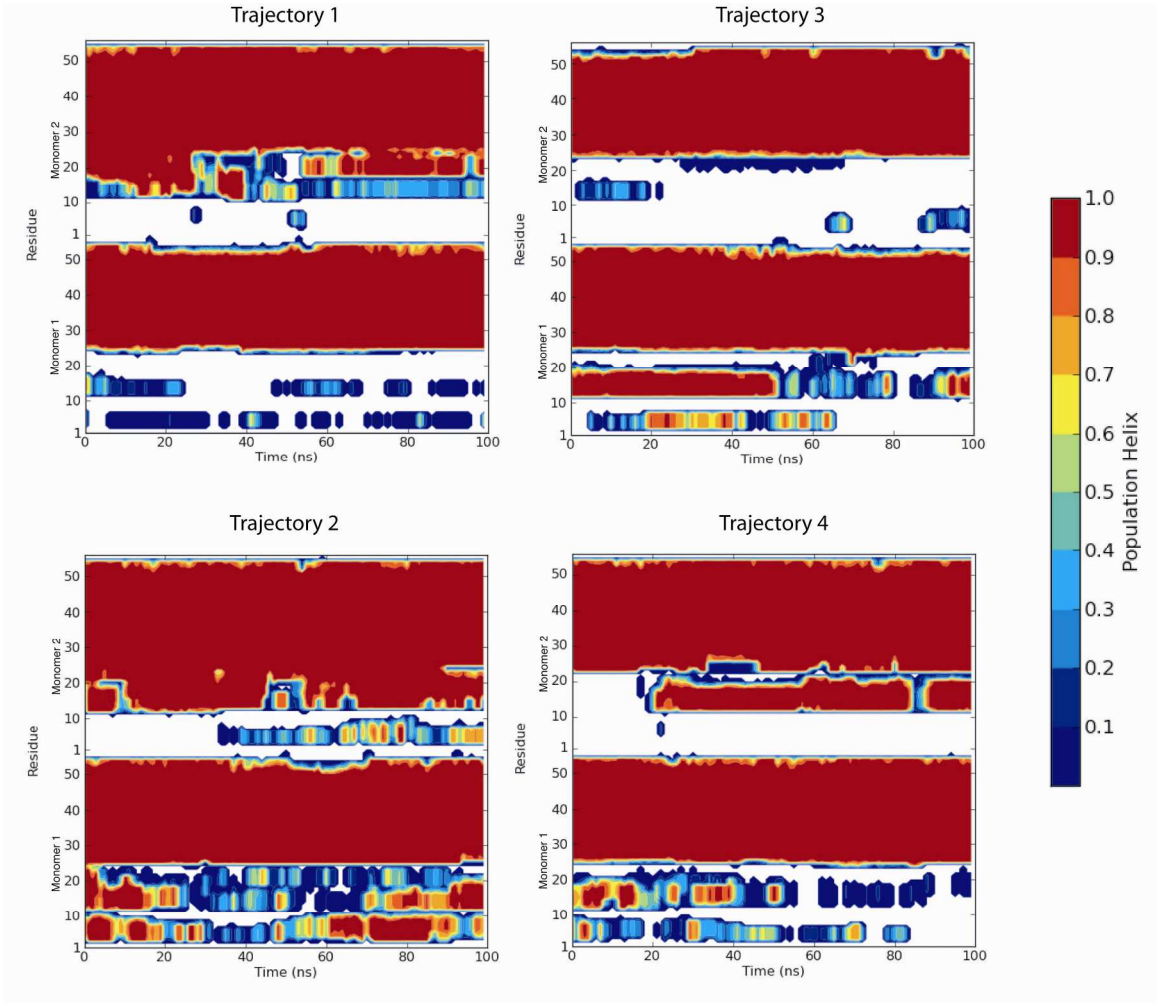

SI Figure 2. Helical fraction of each residue averaged over 1 ns blocks for four 100 ns MD trajectories initiated from starting structures with varying degrees of helicity. Helical conformations were assigned for each MD snapshot using the program STRIDE. The color bar shows the scale. Sections with no helical content are colored white.

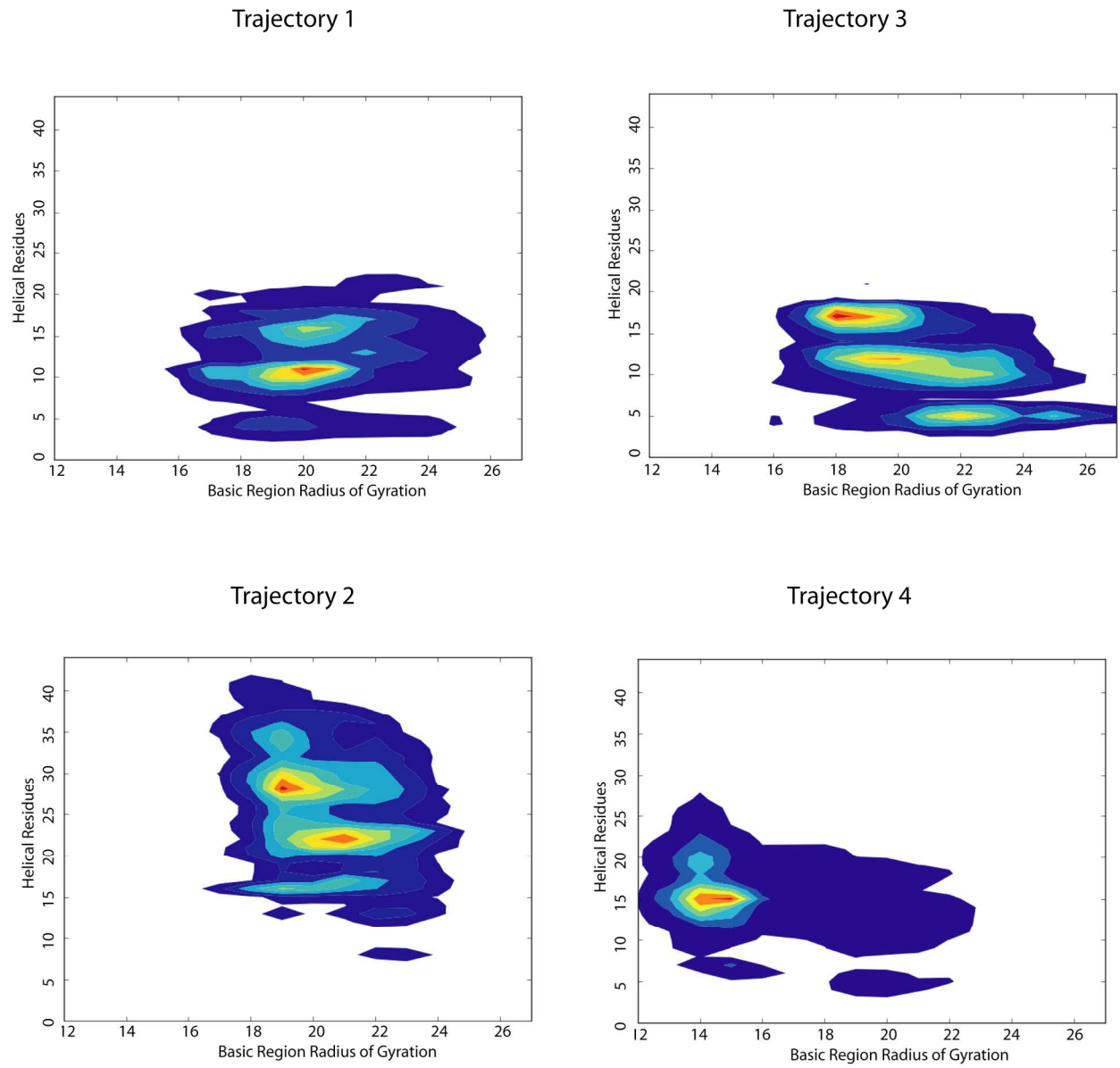

SI Figure 3. Conformational space explored by four 100 ns MD trajectories initiated from starting structures with varying degrees of helicity. Energy landscapes are shown as 2D histograms of the populations of conformations grouped according the basic region radius of gyration and the number helical conformations in the basic region assigned for each MD snapshot using the program STRIDE. The least populated regions of conformational space are colored dark blue, and the most populated regions are colored red.

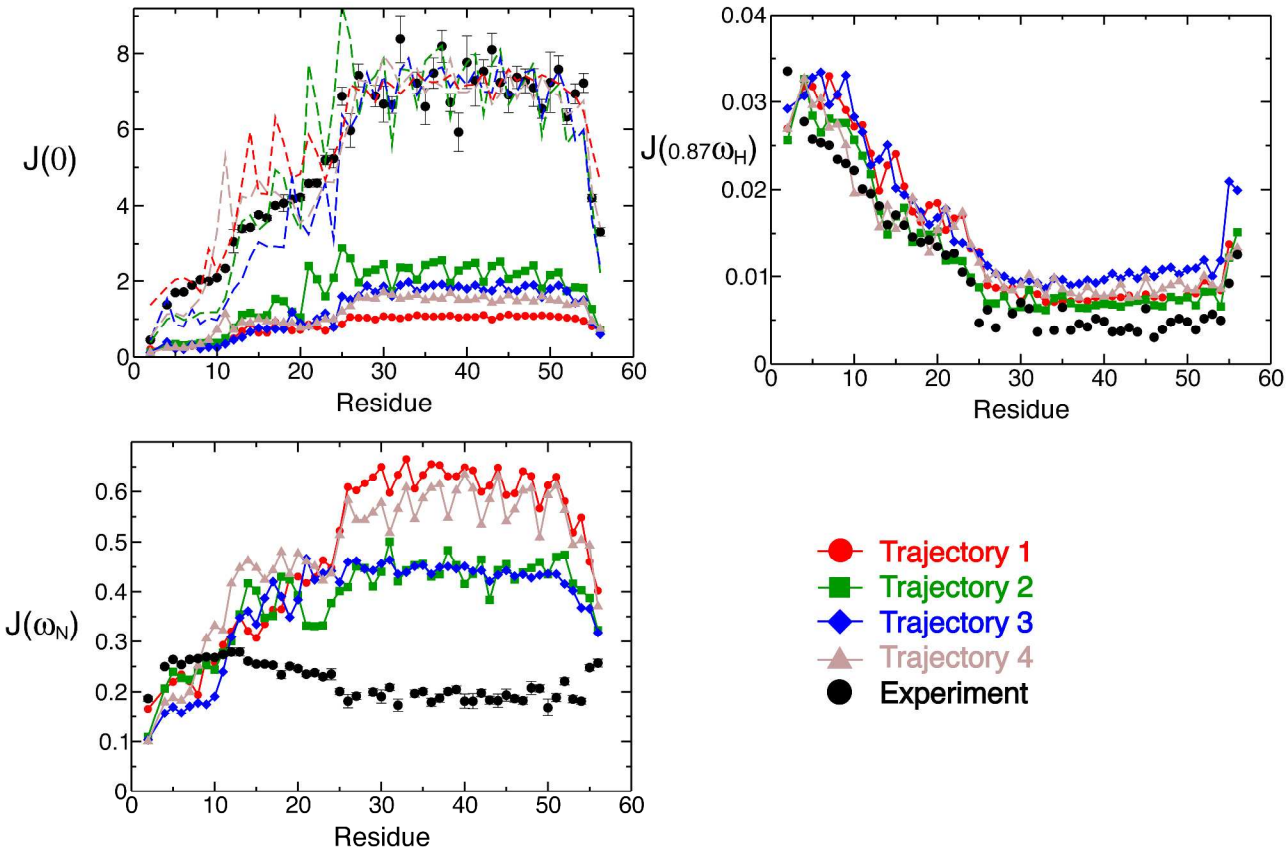

SI Figure 4. Comparison of the values of experimental and simulated spectral density functions ($J(\omega)$) at characteristic frequencies. Simulated spectral density functions were calculated in the "laboratory" frame without performing any alignment of the molecules. For values of $J(0)$, raw values are displayed as symbols and solid lines. Rescaled values, with scaling factors chosen to match the average experimental values of the coiled coil, are displayed as dotted lines to better illustrate the correlation with experimental values.

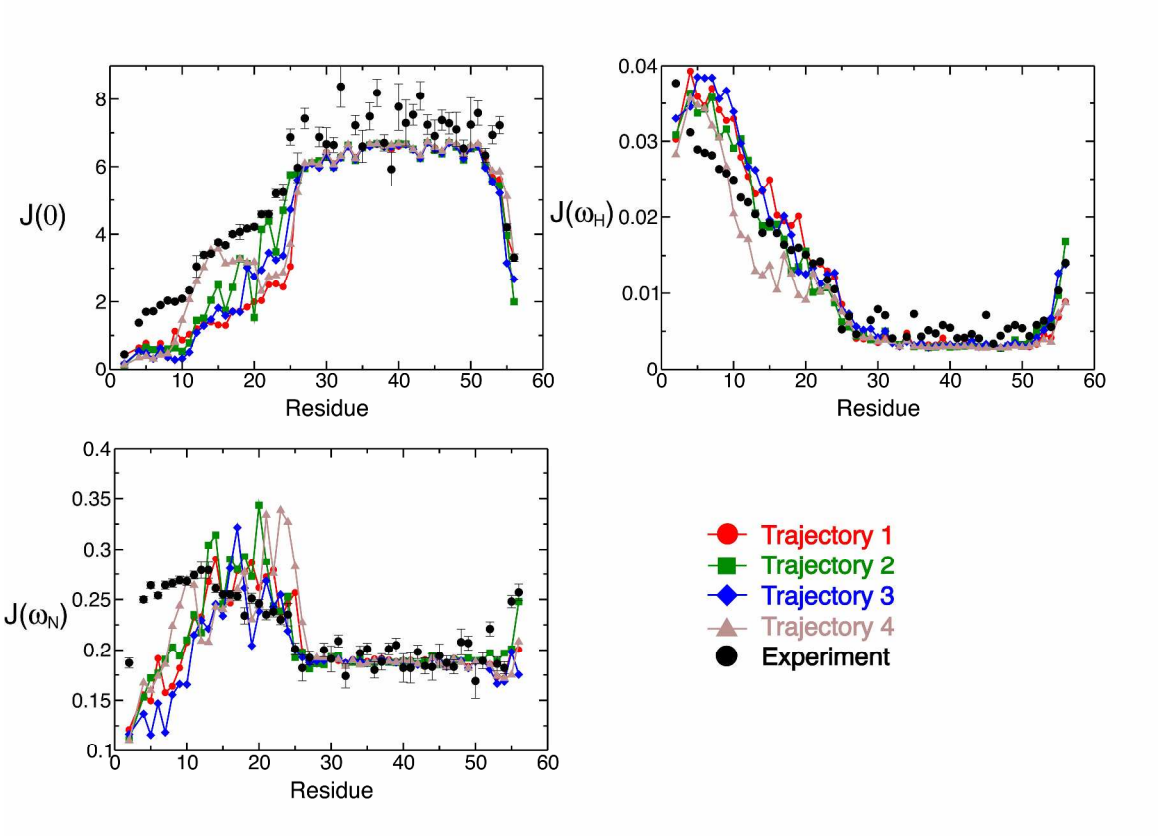

SI Figure 5. Comparison of the values of experimental and simulated spectral density functions ($J(\omega)$) at characteristic frequencies. Simulated spectral density functions were calculated for "internal" motions after superposition of the backbone atoms of the leucine zipper (residues 26-54 of both monomers). To account for the effects of the rotational diffusion of the internal reference frame, all amide bond vector autocorrelation functions were multiplied by an exponential decay with a correlation time of 18.9 ns prior to discrete fourier transformation

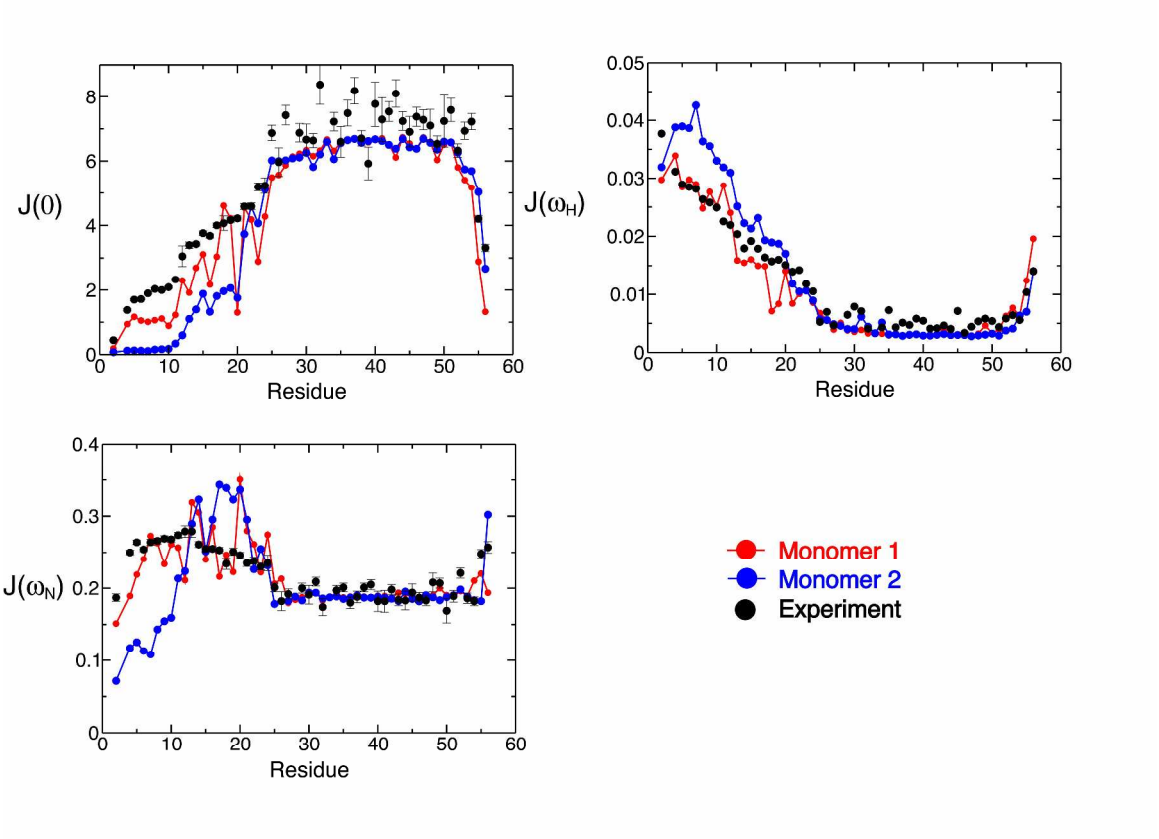

SI Figure 6. Comparison of the values of experimental and simulated spectral density functions ($J(\omega)$) at characteristic frequencies for each monomer of Trajectory 2. Simulated spectral density functions were calculated for "internal" motions after superposition of the backbone atoms of the leucine zipper (residues 26-54 of both monomers). Monomer 1 forms persistent tertiary contacts between residues in H2 and the leucine zipper for the entire trajectory, and contacts between H1 and the leucine zipper for the last 30ns of the trajectory, while monomer 2 does not form any stable tertiary contacts.

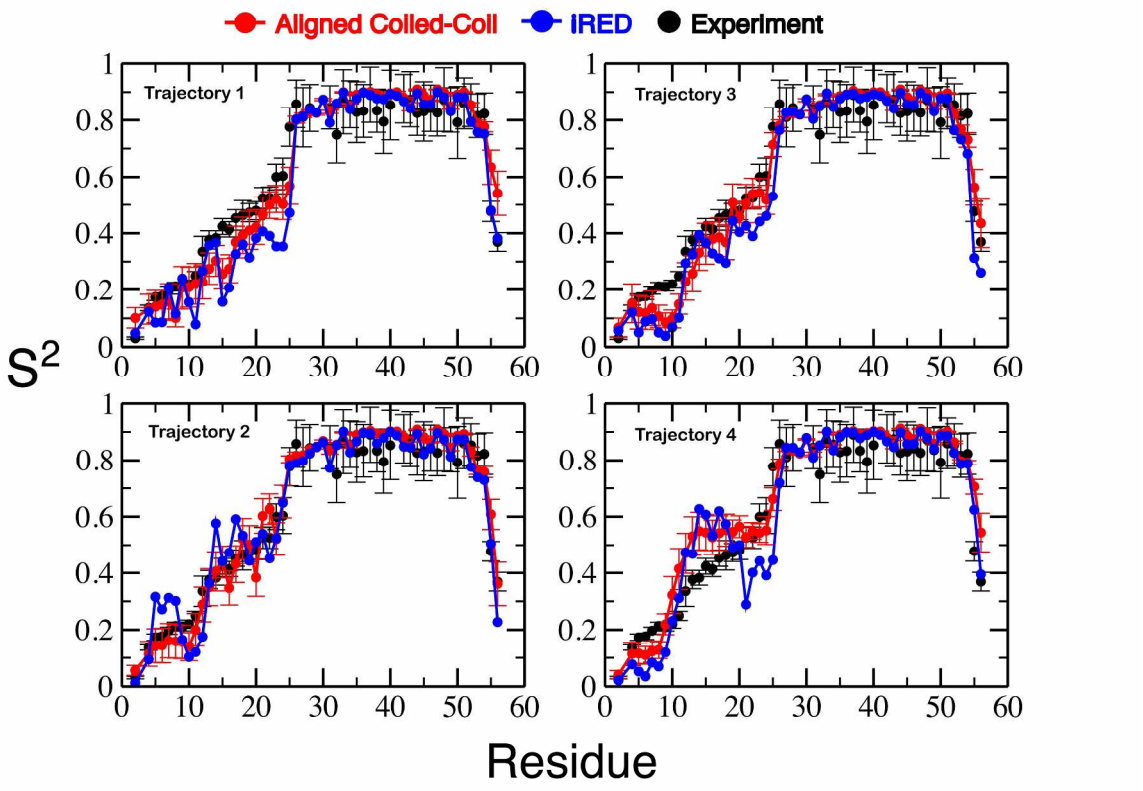

SI Figure 7. Comparison of experimental and simulated generalized order parameters (S^2) calculated after superposition of backbone atoms of the leucine zipper (red) and calculated using the iRED method (blue).

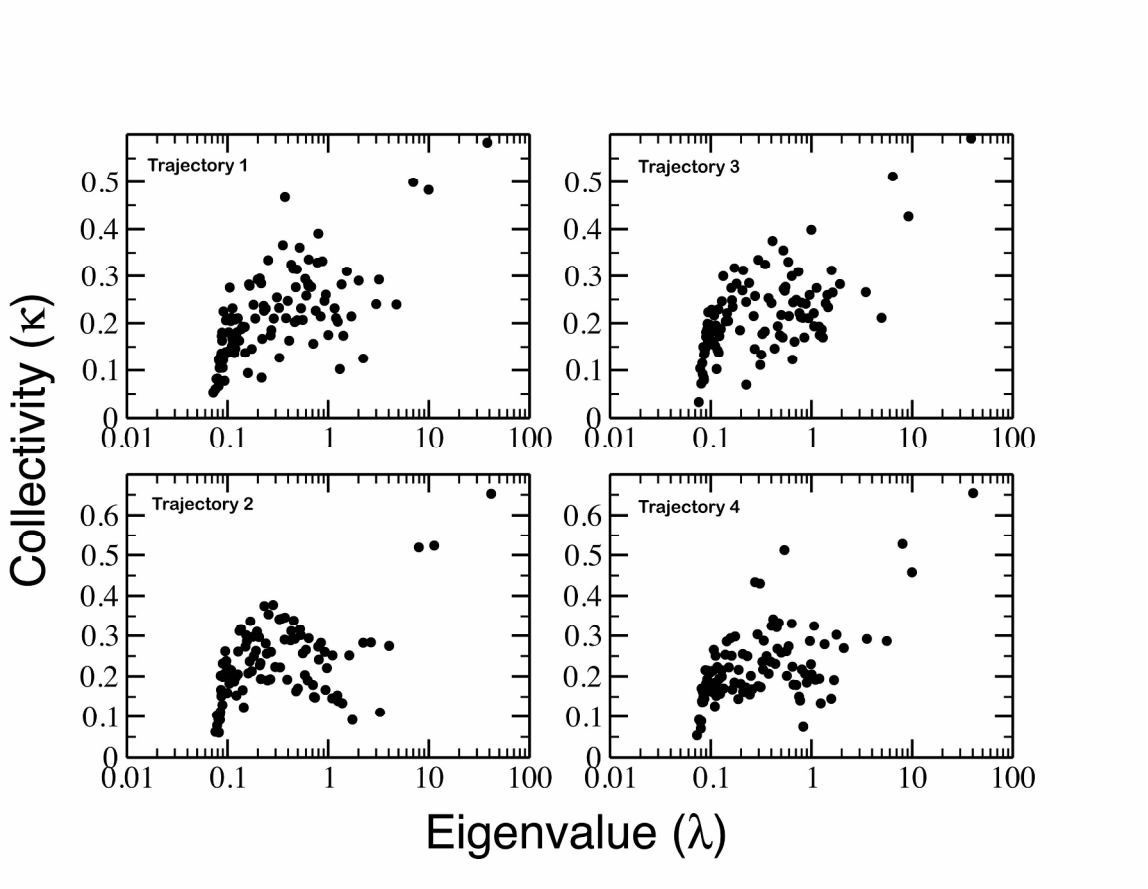

SI Figure 8. Mode collectivities (κ) vs. Eigenvalues (λ) for the eigenmodes calculated in the iRED analysis of each trajectory. Separability of overall tumbling and internal motions results in a large gap between the mode amplitudes λ of the five largest eigenmodes and the remaining eigenmodes. The trajectories examined here do not exhibit such a gap, which is expected based on the fast time scales of overall tumbling observed in these simulations (2.7-6.3 ns) compared to the experimentally determined rotational diffusion constant of 18.9 ns.